Chapter 2

Theory

2.1 Thermal spray process

Thermal spray processes have been used as method of repairing, rebuilding, and retrofitting machine components, restoring original dimensions, or applying corrosion-resistance metals to varius items of infrastructure, such as bridges, pillings, and lock gates. Because of growing interest and continued scientific pursuit among the materials community, thermal spray processes are now widely accepted by many industrial sectors. The success of an application in thermal spray is based on technical and commercial benefits. These include improved technical performance (reliability), longer maintemance intervals, reduced repair times, increased deposit efficiency/deposition rate, and lower overall application cost. Thermal spraying and the many materials applied as coatings have grown to include numerous applications. The aerospace industry is probably the first and the largest user of thermal sprayed coatings. The aerospace industry was manufacturing segment that reconized the great utility and value of thermal spray coatings and was widely responsible for driving the development and confidence in thermal spray processes and coatings. The automobile industry have relied on thermal spray processs for more than 30 years as wear and scruff resistant coatings on piston rings, selector forks and syncro cones. The developments which have taken place in the printing industry in recent years have

created a need for precise laser engraving of anilox rolls. From its humble beginnings, the thermal spray industry has truly grown into an important, global industry [7].

Thermal spraying is a group of processes wherein feedstock material is heated and propelled as individual particles or droplets onto a surface. The thermal spray gun generates the necessary heat by using combustible gases or and electric arc. As the materials are heated, they are changed to a molten state and are confined and accerlerated by a compressed gas stream to the substrate. The particles strike the sucstrate, flatten and form thin splats that conform and adhere to the irregularities of the prepared substrate and to each other. As the sprayed particles impinge upon the surface, they cool and build up, splat by splat, into a laminar forming the thermal spray coating. Figure 2.1 illustrates a typical coating cross section of the laminar structure of oxides and inclusion. The coating that formed is not homogenous and typically contains a certain degree of porosity and in the case of sprayed metals, the coating will contain oxides of the metal. Feedstock material may be any substance that can be melted, including metals,metallic compounds, cements, oxides, glasses and polymers. Feedstock materials can be sprayed as powders, wires or rods. The bond between the substrate and the coating may be mechanical, chemical or metallurgical or a combination of these. The properties of the applied coating are dependent on the feedstock material, the thermal spray process and application parameters [8].

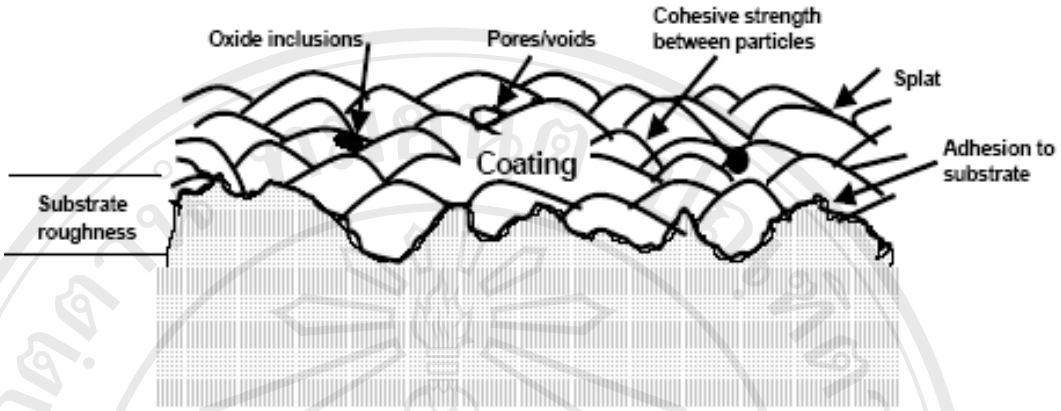

Figure 2.1 Typical cross section of a thermal spray coating [8]

In principle, powders, rods, and wires can be used as spraying materials. Metals and alloys in the form of rods or wires are commonly used in arc spraying (AS) and flame spraying (FS). Powders of metals, alloys, ceramic oxides, cermets, and combides are often used in thermal spraying to produce a homogeneous microstructure in the resulting coatings. In most cases, the sprayed surface should be degreased, masked and roughened prior to spraying to maximize the bonding strength between the coating and the substrate material. A variety of thermal spray techniques have been developed since the 1900's. Today, flame spraying (FS), plasma spraying (PS), arc spraying (AS), detonation gun (D-gun) spraying, and high velocity oxy-fuel spraying (HVOF) are widely used to produce various coatings for different industrial applications. Thermal spraying processes may be divided into two categories according to the method of heat generation namely electrical and combustion heating (Figure 2.2) [9].

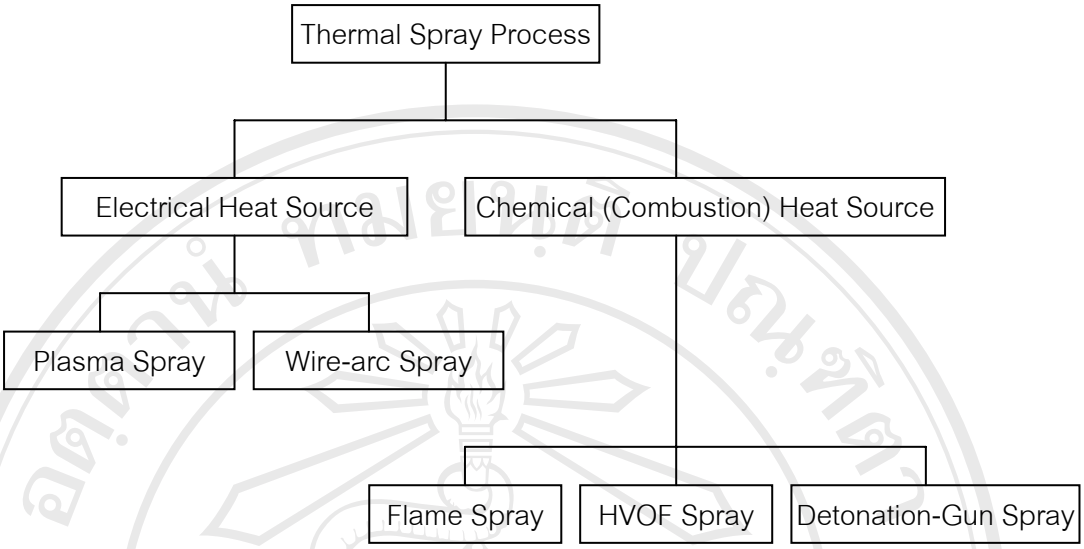

Figure 2.2 Diagram show categories of thermal spray process [9].

2.1.1 Flame spraying

The flame spraying process is characterized by very low capital investment, high deposition rates and efficiencies, and relative ease and cost of maintenance. In general, flame sprayed coatings exhibit higher porosity, lower bond stength, a narrow working temperature range, and higher heat transmission to substrate than other thermal spraying process.

The most commonly used combustible gases in fame sprayed process are oxyacetylene and oxyhydrogen. The flame temperature ranges from 3000 to 3350 °C depending on oxygen-fuel gas ratio. This process utilizes combustion flame as heat source to melt the coating material, available in wire, rod, or powder form. The term metallizing is also used to describe a flame spraying process which involves the use of metal in wire form. Figure 2.3 and 2.4 shows schematically the wire and powder flame spraying processed. In the wire flame spraying process, shown in Figure 2.3 the

source comprises a nozzle, through the center of which wire is fed at a controllable rate into the flame, which melts the wire tip. Compressed air is fed through the particles onto the substrate. The wire tip is continuously heated to its melting point and then is broken down into particles by the stream of compressed air. Any metal that can be down into wire form and will melt in the environment of combustion flame can be sprayed. In powder flame spraying process, shown in Figure 2.4, the powder material is held in a hopper atop the gun and is gravity-fed into the gun, where it is picked up by a carrier gas and carried to the gun nozzle. Here the jet arrangement at the gun nozzle. This process is also call powder welding. The powder flame spray process extends the choice of materials to encompass those which cannot be produced in wire or rod form [10].

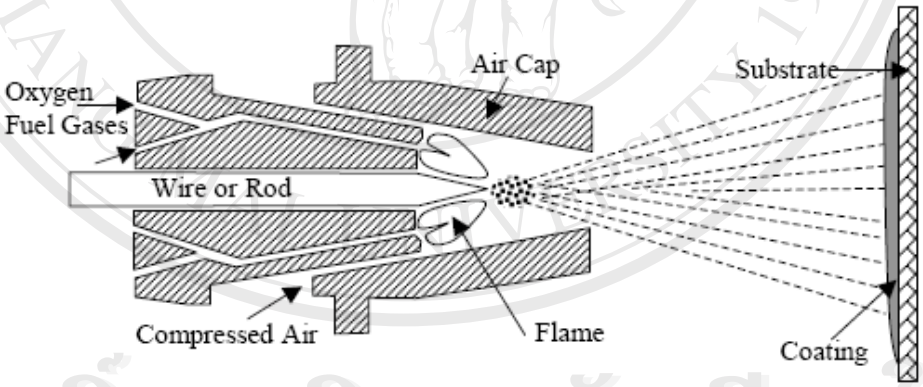

Figure 2.3 Cross section of a wire or rod flame spray gun [10].

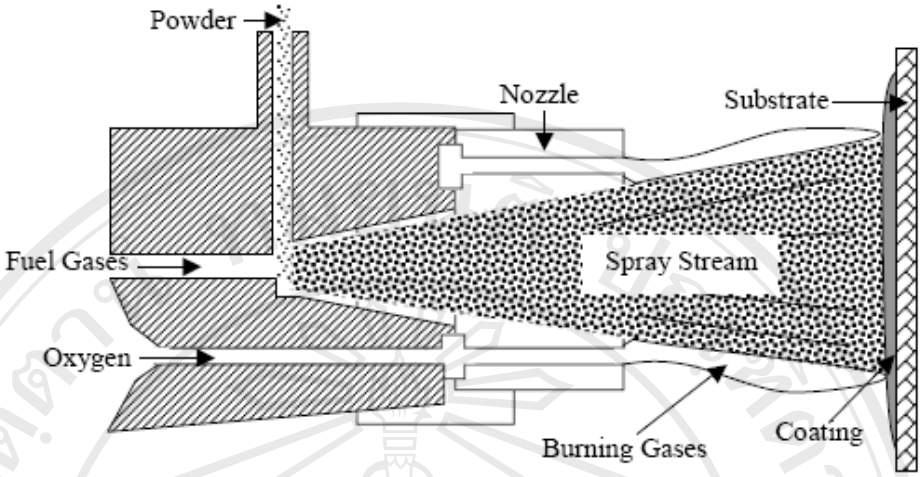

Figure 2.4 Cross section of a powder flame spray gun [10].

2.1.2 High velocity oxy-fuel spraying (HVOF)

The HVOF (High Velocity Oxy-Fuel) thermal spray process is one of the newest methods of thermal spray, and another form of the flame spraying process, as mentioned in point one of this section, but utilizing only powder as the coating material rather than wire or rod. The HVOF (High Velocity Oxygen Fuel) Thermal Spray Process is basically the same as the combustion powder spray process (LVOF) except that this process has been developed to produce extremely high spray velocity. One method is basically a high pressure water cooled HVOF combustion chamber and long nozzle. Fuel (kerosene, acetylene, propylene and hydrogen) and oxygen are fed into the chamber, combustion produces a hot high pressure flame which is forced down a nozzle increasing its velocity. Powder may be fed axially into the HVOF combustion chamber under high pressure or fed through the side of laval type nozzle where the pressure is lower. Fuel gas (propane, propylene or hydrogen) and oxygen are supplied at high pressure, combustion occurs outside the nozzle but within an air

cap supplied with compressed air. The compressed air pinches and accelerates the flame and acts as a coolant for the HVOF gun. The burning gas mixture is accelerated to supersonic speeds, and a powder feed stock is injected into the flame. Figure 2.5 shows a schematic of a typical HVOF process.

The process minimizes thermal input and maximizes particle kinetic energy to produce coatings that are very dense, with low porosity and high bond strength. The coatings produced by HVOF are similar to those produce by the detonation process. HVOF coatings are very dense, strong and show low residual tensile stress or in some cases compressive stress, which enable very much thicker coatings to be applied than previously possible with the other processes. The very high kinetic energy of particles striking the substrate surface do not require the particles to be fully molten to form high quality HVOF coatings. This is certainly an advantage for the carbide cermet type coatings and is where this process really excels.

HVOF coatings are used in applications requiring the highest density and strength not found in most other thermal spray processes. HVOF has been used extensively to apply wear resistant coatings for applications such as jet engine components. The Corps has conducted an experimental evaluation of HVOF-applied metal alloy coatings for protection against cavitation wear in hydraulic turbines [9, 11].

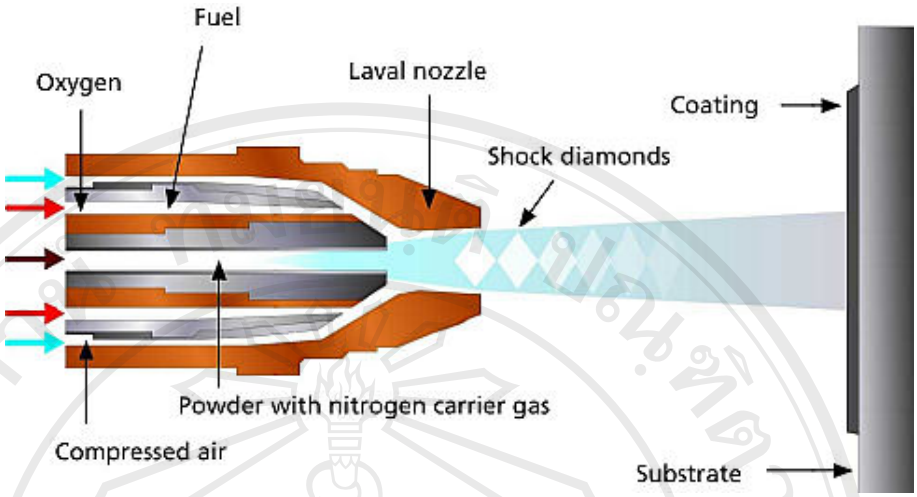

Figure 2.5 Schematic of HVOF spraying process [9].

2.1.3 Detonation-gun spraying (D-gun)

The detonation-gun process is some what similar to oxyacetylene powder flame spraying process. In detonation-gun spraying process, when measured quantities of oxygen, acetylene, and particles of coating material are metered into the firing chamber, a limited spark detonates the mixtures. The resulting detonation is high, approximately 150 dB. Because of this, the denotation consists of heat and pressure waves which create a hot, high-speed gas stream which instantly heats the particles to a molten state (about 4500 °C) and hurls them at supersonic velocity (about 800 ms^{-1}) from the gun barrel to the substrate surface.

The detonation gun, shown schematically in Figure 2.6, consist of a water cooled barrel about 1 m long with an inside diameter of about 25 mm and associates gas and powder metering equipments. A mixture of oxygen and acetylene is fed via the poppet valve into the barrel along with a charge of powder in a carrier gas stream. The gas mixture is then ignited by an electric discharge or a spark plug. Detonation or

shock waves, which follow within milliseconds after ignition, accelerate the powder to the substrate at about 800 ms^{-1} while heating is close to or above its melting point. After the powder has exited the barrel, a pulse of nitrogen gas purges the barrel. The cycle is repeated about 4 to 8 times per second. The uniform, closely packed, laminar structure of a detonation gun coating, produced by extremely high-velocity hot gas stream, results in hardness, density, and bond strength higher than can be achieved with conventional plasma of flame spray processes [12].

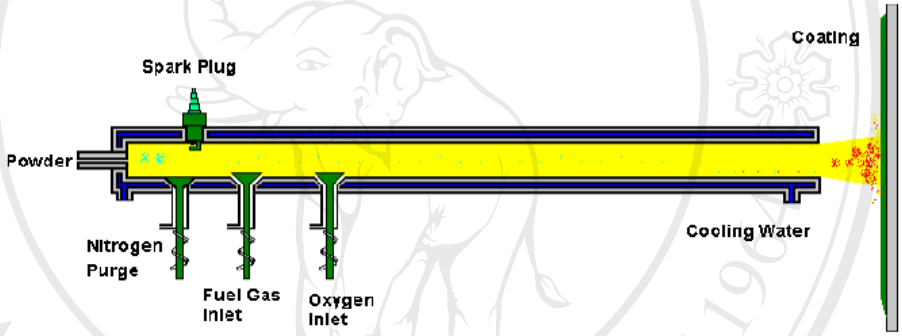

Figure 2.6 Schematic of detonation-gun spraying process [9].

2.1.4 Plasma spraying

In this process a dc electric arc is struck from a high-frequency arc stater between a central (tungsten) electrode in the torch and a water-cooled (copper) nozzle, which forms an anode, while a stream of inert gased (either argon or nitrogen, sometimes with the addition of other gased such as hydrogen or helium) is passed through this arc. In the plasma arc spraying process (simply known as plasma spraying), the thermal energy of an electric arc (usually operating at either 40kW or 80kW) together with a plasma forming gas, either nitrogen or argon, is utilized in the melting and projecting of the deposit material at high velocities (~600m/s), onto a

substrate. The main use of this system is to generate high temperatures, reaching 16,000°C with some systems for the deposition of materials with high melting. The deposit material is generally in powder form and requires a carrier gas to feed the powder into the combustion chamber, as shown in Figure 2.7. Because of the high propulsion of the individual particles, high bond strengths and high density may be achieved in the coatings [12].

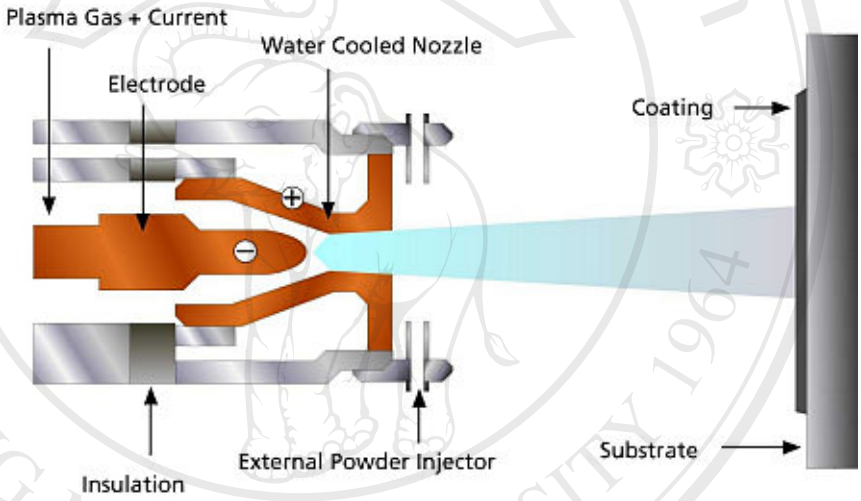

Figure 2.7 Schematic of plasma spraying process [9].

2.1.5 Arc wire spraying

The electric arc spraying process is used to spray metals in wire form. This spraying process along with the wire flame spraying process is also referred to as the metallizing process. This process differs from other thermal spraying processed in that there is no external heat source, such as gas flame or electrically induced plasma. Figure 2.8 shows a schematic of the electric arc spraying system.

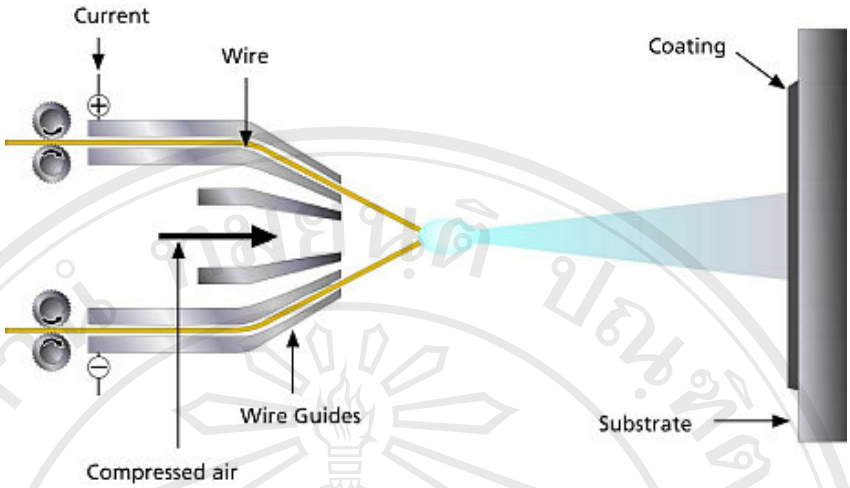

Figure 2.8 Schematic of electric arc spraying system [8].

Arc spray use to apply electrically conductive materials including metals, alloys and metal-metal oxide mixtures. Wire electric arc spraying used two electrically conducting wires as feedstock. In arc spraying, an arc between two wires is used to melt the coating material. A continuous direct current arc melts the tips of the advancing wires, and a high velocity gas acts to atomize the melted wires and accelerate the fine particles to the substrate. Compressed gas, usually air, is used to atomize and propel the molten material to the substrate. The two wires are continuously fed to the gun at a uniform speed. A low voltage (18-40 volts) direct current (DC) power supply is used with one wire serving as the cathode and the other as the anode. Figure 2.9 shows a typical arc spray system comprised of a DC power supply, insulated power cables, a wire feed system, a compressed air supply, controls and an arc spray gun. Coating quality and properties can controlled by varying the atomization pressure, air nozzle shape, power, wire feed rate, traverse speed and standoff distance [10].

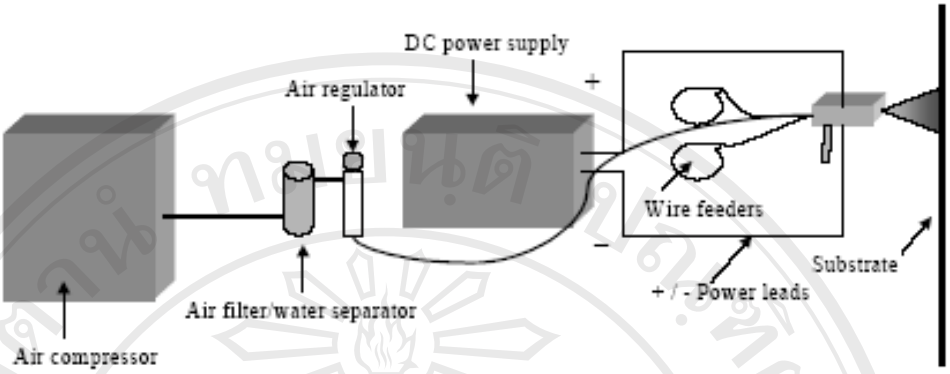

Figure 2.9 Typical two-wire arc spray system [10].

Electric arc spraying offers several advantages over other thermal spray processes. Differences exist in the resultant coatings, due to different heating processes involved. Substrate heating is lower than in other processes due to primarily to the absence of a flame toughing the substrate. Under comparable conditions, the adhesion of arc sprayed coatings is higher than that of flame sprayed coatings. A less expensive wear surface can be deposited by using this process. The electric arc gun is lightweight and is easily held in the hand. The electric arc spraying process can be used to produce coating of mixed metals, often termed psedo-alloy, by feeding dissimilar wire [12].

2.2 Spraying materials

Materials that can be plastically formed either in the solid or liquid state can be deposited. Where heating is involved, only those materials that remain stable upon heating can be sprayed. Instability may refer to oxidation or decomposition of the

material. These materials may, however, be deposited in the form of composites where a secondary material is used to protect the unstable or reactive material. Spraying into a special atmosphere, use of a metallic or polymeric binder to form a composite, or encapsulation of these powder are means of protecting the thermally sensitive materials.

The development continued by varying the type of deposition materials (powder, wire and rod) and combustion temperatures [13]. In general, any material which does not decompose, vaporize, sublimate, or dissociate on heating, can be thermally sprayed. Consequently a large class of metallic and nonmetallic materials (metals, alloys, ceramics, cermets, and polymers) can be deposited by thermal spraying. For wear resistance applications, coatings of hard metals, alloys, intermetallics, and nonmetals are common used. Thermal spray feed stocks can take several forms which are suited to various materials such as:

· Powder – plastic, metal, composite, ceramic

· Wire – metal, composite

· Rods – ceramic

· Liquid

Powders are available for flame, plasma and HVOF spraying. Materials sprayed include plastics, metals, carbides and ceramics, and many compositions can be sprayed by all four processes. The optimum powder specification depends on the process, and includes consideration of particle size and distribution, morphology and

manufacturing route. Wires are principally used in arc spraying, which requires a continuous, electrically conducting consumable. Most wires are solid in form, and based on aluminium, zinc or steel compositions. In common with welding consumables, cored wires (containing ceramic or alloying material) are now available. Some flame spraying systems also use wire consumables, principally for spraying zinc or aluminium [14].

A large literature exists on the wide diversity of materials used as thermal spray feedstock. Many different types of ferrous alloys are thermal sprayed, including stainless steel and cast iron. In recent years, and very important both industrially and scientifically, intermetallic alloy powders have been plasma sprayed in environmental chambers, for example, on niobium as oxidation-resistant protective coatings and as free-standing forms. Wide ranges of cermets are available, that is, blends of metals and ceramics, which when plasma sprayed produce very high strength deposits. Novel ceramics, glasses and various high performance materials have begun to be available. These materials will be the basis for new plasma spray applications in the future. Metal alloys and ceramics differ in the manner in which they are fed into thermal spray guns. Metals are employed as powders and wires, and ceramics are used as powders and sintered rods (the latter, for special proprietary guns), usually 1/4 inch in diameter [15].

2.3 Welding process

The number of different welding processes has grown in recent years. These processes differ greatly in the manner in which heat, pressure, or both heat and pressure are applied, and in the type of equipment used. The most popular processed

are gas metal arc welding (GMAW), oxyacetylene welding (OAW), shielded metal arc welding (SMAW), gas tungsten arc welding (GTAW), and flux core arc welding (FCAW) [16].

The freedom from spatter associated with the gas metal arc shield (GMAW or MIG Welding) process results from a unique mode of metal transfer as shown in Figure 2.10. This process is identified by the pointing of the wire tip from which very small drops are projected across the arc gap to the molten weld pool. There are hundreds of drops per second crossing from the wire to the base metal. These drops are propelled by arc forces at high velocity in the direction the wire is pointing. Since the drops are separated and directed at the molten weld pool, the process is spatter free. This spray transfer process requires three conditions: shielding gas, polarity and a current level.

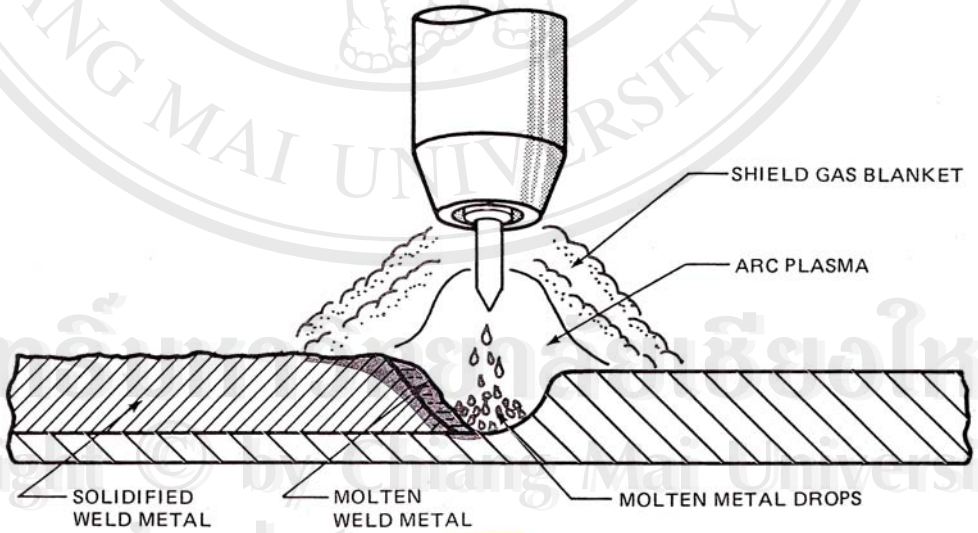

Figure 2.10 Gas shielded metal arc welding (GMAW) [16].

2.4 Wire (weld wire and arc wire)

Stainless steel weld wire consist of chromium content provides corrosion resistance, while its nickle content produces the tough microstructure. These steels are relatively easy to weld, and a large variety of electrode types are variable. The most widely used stainless steels are the chromium-nickle content as 18/8, 25/12, 25/20, and so on. For example, 18/8 contains 18% chromium and 8% nickle, with 0.08% to 0.20% carbon. Some stainless steels types have special low carbon variation. These carbon stainless steels are the same as the base type but with much lower carbon content. To identify the low carbon from the standard AISI number the “L” is added as a suffix. See examples 316 and 316L in Table 2.1. In welding with the metal arc process, direct current is more widely used than alternating current. Generally, reverse polarity is preferred where the electrode is positive and the workpiece is negative. The diameter of electrode used to weld stainless steel that is lower than 3/16 in.(4.8 mm) Stainless steel is gas weldable using a special stainless steel flux. The filler metal must be properly matched to the base metal. The stainless steel filler welding rods are identified by the American Iron and Steel Institute (AISI) stianless steel number prefixed with the letters E, for electrode, and R for welding rod. Both letters are sometimes used because the same wire chemistry is used for gas metal arc welding. Table 2.2 list some of the stainless base metals and the stainless filler metals derived from them [16].

Table 2.1 Comparison of standard grade and low carbon stainless steels [16]

Nominal Comparison of Stainless Steels						
AISI Type	**Nominal Composition %**					
	C	**Mn Max**	**Si Max**	**Cr**	**Ni**	**other**
304	0.08 max	2.0	1.0	18-20	8-12	
304L	0.03 max	2.0	1.0	18-20	8-12	
316	0.08 max	2.0	1.0	16-18	10-14	2.0-3.0 Mo
316L	0.03 max	2.0	1.0	16-18	10-14	2.0-3.0 Mo

Table 2.2 Major stainless steels and filler metals [16].

Base Metal AISI No.	**AWS Filler No.**	**Common Uses**
302	ER308 or ER308L	General fabrications, caninets
304	ER308 or ER308L	General utility, brackets, braces
308	ER308 or ER308L	Food storage, trailer bodies
309	ER309	Furnace parts, mufflers
310	ER310	Heat treating fixture, valve casting
316	ER316 or ER316L	High temperature and chemical equipment

Materials for arc spraying is all electrically conductive. There are traditionally Zn and Al wire, but core wires are now also in extensive use. The core wires are composed of two phase and typically the sheat makes approximately 50% of the total composition. Diameter is typically in the range 2-5 mm [2]. Arc wire brings the operational simplicity and portability of MIG welding technology to the field of thermal spray. The result is a system capable of applying a quality surface treatment at virtually any location. Additionally, the high feed stock capacity of the arc wire system makes it ideal for coating large areas such as structural surfaces and large rolls [17].

2.5 Coating formation

In the spraying process, particles become superheated and projected towards a substrate at high velocities. Depending on the melting temperatures of the particle relative to the flame temperature, the particle may be molten, semi-molten or solid when it impacts a substrate or pre-coated surface. Particles may be solid, liquid, vapour or a combinations of all three, as they exit the gun, hence the state of an individual particle impacting a substrate. The goal while optimizing the spraying parameters is to ensure that all particles impacting the substrate are molten and have a maximum velocity possible.

The common feature of thermally sprayed coatings is their lamellar grain structure, resulting from rapid solidification of small globules, flattened from striking a colder surface at high velocities. Figure 2.11 shows a schematic of the formation of a splat from its globular form. Initially, the particle is melted and propelled out from the gun in the form of a sphere then, at its first contact with the substrate, the impact

creates a shock wave inside the lamella and in the substrate. Post-impact the particle forms into a pancake shape (associated with moderate particle velocities and moderate heat contents) lamella (or splat), shown in Figure 2.12 (a), or a flower type (connected with an elevated velocity of the particle and an elevated heat content) lamella, as shown in Figure 2.12 (b), when the solidification process takes place. The behavior of the particles on impact have been researched intensively by various authors either using numeric or analytical models [18,19]. The shape and structure of the splat gives a lot of information about certain spray parameters, such as whether the correct spraying distance have been utilized during deposition [20-22].

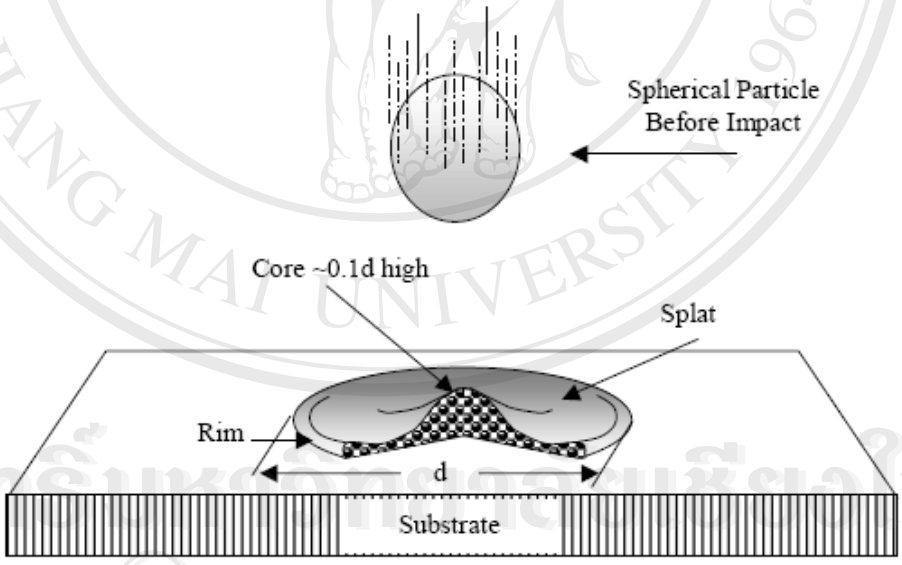

Figure 2.11 Schematic diagram of spherical impinged onto a flat substrate [18].

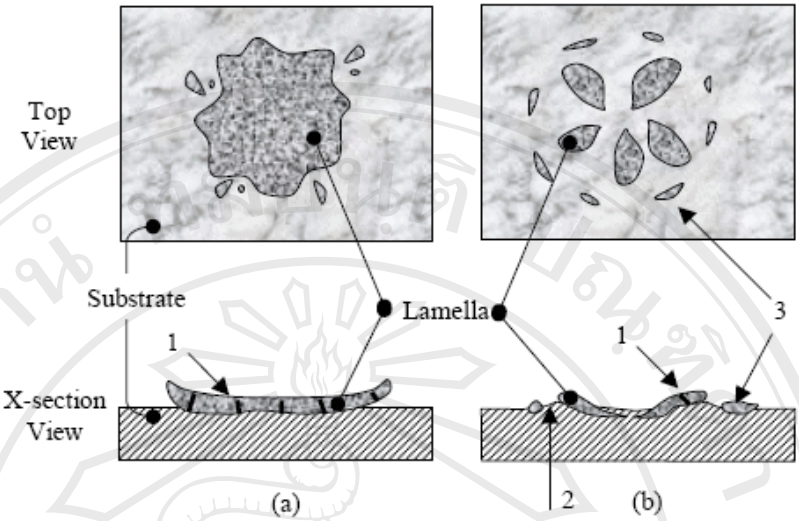

Figure 2.12 Two morphological forms of lamellae splashed on the substrate (a) Pancake, (b) Flower [18]

This solidification process for each individual droplet is common to virtually all microstructures in sprayed materials, and the layering of these individual particles on top of each other leads to a coating. A coating is the build up of individual particles which strike a substrate. Particles can be fully or partially melted at the moment of impact, depending on their melting temperatures. The solid particles may rebound or remain weakly connected to the rest of the coating, reducing its strength. That is why careful optimization of spray parameters is necessary to eliminate such problems. As the spray torch applies the one pass of spray, this deposit a layer of 5 - 15 lamellae thickness, depending on the processing parameters such as powder feed rate, spray distance, particle size and the torch's linear speed. Generally in thermal spraying technologies, the spray gun is allowed to make several passes across the work-piece in order to build-up a coating. Meanwhile, the layer deposited by the first pass may be submitted to oxidation (for oxidizable materials) and cooling. On the second pass, the

temperature of the first layer (which may be partially solidified) cools the second layer due to the difference in temperatures between the first and second layer. The final coating may comprise of 5-200 passes of deposited material. Afterwards, the coating is allowed to cool down to room temperature, during this period thermal stresses generate, often leading to crack formation in the coating or separation from the substrate.

Once a molten or semi-molten particle strikes the substrate or previously deposited material, solidification starts. Depending on the traverse speed of the gun and on the structure of the particle (explained in the last section) a columnar deposit structure (Figure 2.13) is formed. It has been observed [2], that the deposit structure changes to a .brick wall. (Figure 2.14) type structure, where a low rate of heat removal is experienced between the particle and the adjoining material interface, due to substrate oxidation and/or surface roughness. In either case the solidification within each lamella will repeat itself as the coating builds up to the required thickness.

The formation of a thermal spray results from the build-up of individual molten or semi-solid particles that strike on the surface of the substrate. Particle impingement at the substrate surface is a dynamic process which combines particle at the moment of impact influences the grain size and phase composition of the coating. Thereby, the phenomenon of melted or semi-melted particles impacting on the substrate is crucial in determining the coating characteristics such as porosity, inclusions, and chemical segregation [23].

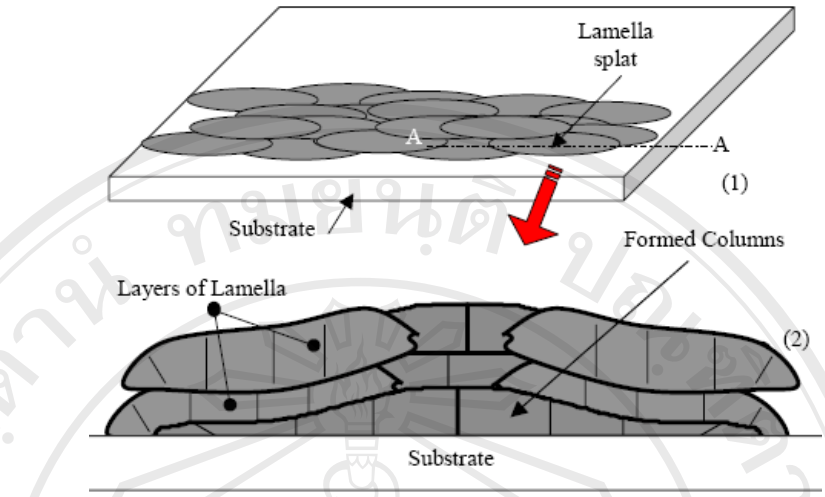

Figure 2.13 A cross-section of lamella splat in diagram (1) is shown in diagram (2), which represents the possible microstructure of lamellae resulting from solidification (columnar) [2].

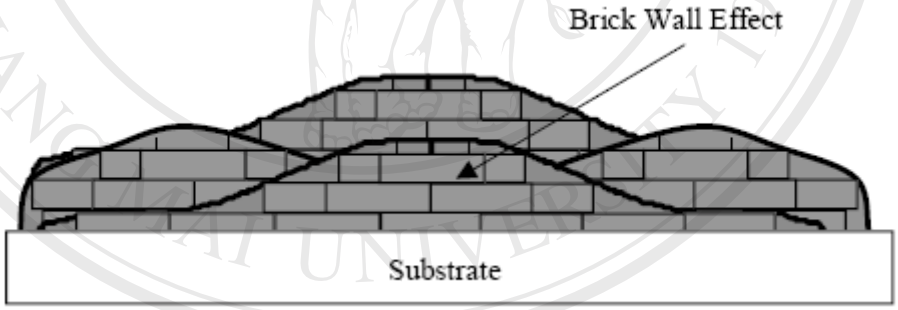

Figure 2.14 Another cross-section through a lamella, showing a Brick-wall type microstructure resulting from solidification [2].

Splat formation is one of the most important fundamental topics involved in thermal spray technology. When splat deposited by molten droplet on a flat substrate surface at an ambient atmosphere in thermal spraying, the splashing results in the formation of the splat in an irregular morphology [24].

2.5.1 Flattening degree

The flattening degrees were estimated using the average diameter of splats and spray particles for different spray conditions. As a thermal spray coating is constituted of splats, the performance of the coating can be determined by the lamellar structure of the coating and the microstructure of individual splats [25]. The flattening degree is defined as the ratio of the diameter of the splat to the diameter of starting droplet, Therefore, it is essentially important to understand how the droplet conditions, including velocity, temperature and size, influence the flattening degree of a spray molten droplet.

Relationships links between the diameter of an impinging particle and the diameter and the thickness of the resulting splats as follows:

$$H = \frac{2}{3} \cdot \frac{d^3}{D^2} \qquad (2.1)$$

Where D and H, respectively, represent the splat diameter and splat thickness; and d is the diameter of the impinging particle. In the following calculations, the thickness of the splat was assumed to be equal to 1/12 of the diameter of the impinging particle [26]. By rearranging Equation**,** the diameters of impinging particles having led to the formation of splats were defined as:

$$d = \sqrt{\frac{1}{8}} \cdot D \qquad (2.2)$$

The recent papers were devoted to investigate droplet flattening onto a smooth surface. Such models allowed the calculation of the flattening degree $\xi = D/d_p$, where D is the diameter of the splat, assumed to be cylindrical, and d_p is the diameter of the impacting droplet.

2.5.2 Shape factor

Particle shape is defined here as a 'shape factor' that attempts to quantify shape as a single number. This is not easy and there have been many attempts in the past. The definition of shape factor used in this case is based on the measurement of the length of a large number of particle radii passing through the geometric centre (similar to the two used for aspect ratio determination). Firstly the root mean square (RMS) deviation in particle radii length is found. This may be defined mathematically as:

$$r_{rms.d} = \sqrt{\frac{(r_{\max} - r_{mean})^2 + (r_{mean} - r_{\min})^2}{2}} \qquad (2.3)$$

Where $r_{rms.d}$ is the RMS deviation of radii lengths and r_{min}, r_{mean} and r_{max} are, respectively, the minimum, mean and maximum radii lengths. It should be noted that the RMS deviation is the RMS value of the deviation in radii lengths and not the RMS radius length. The shape factor (S_F) itself can now be defined as $r_{rms.d}$ normalized to the mean length, i.e.:

$$S_F = \frac{r_{rms.d}}{r_{mean}} \qquad (2.4)$$

This definition of shape factor has been found to give consistent results and is simple enough to allow high performance processing. It is also of greater relevance to irregular shaped particles than other shape factors (or 'circularity' definitions) that are commonly defined in such a way as to give a result equal to one for a perfect circle – as the shape deviates from the circular the resulting figure becomes smaller. This is acceptable where objects are expected to be circular and any deviations from this are small but, when working with particles that are consistently irregular in shape, the results will consist of very small numbers. Perfectly circular particles will generate a value of zero and this figure will increase with the deviation from circular of the particles. This means that there is no limit to the variations in shape that the present definition will allow to be highlighted. It will, in theory, produce a single, unsigned, figure that can vary from zero to infinity which describes particles varying from a perfect circle to infinitely non-circular (i.e. a straight line)[27].

Different shape factors were used in order to quantify the phenomena; in particular the equivalent diameter, E.D., defined as the diameter of a circle with the same area as the selected feature; the elongation factor, E.F., defining the non-circular nature of a selected feature, unity being a perfect circle; and the degree of splashing, D.S., characterizing the importance of the splashing phenomenon (i.e., peripheral projection of material at the impact); unity resulting from an absence of such projections. Equation (2.5)-(2.7) present the mathematical definitions of these shape factors [26, 28], schematically illustrated in Figure 2.15.

$$E.D. = \left(\frac{4 \cdot A}{\pi} \right)^{1/2} \tag{2.5}$$

$$E.F. = \frac{n}{4} \cdot \frac{L^2}{A} \tag{2.6}$$

$$D.S. = \frac{1}{4\pi} \cdot \frac{P^2}{A} \tag{2.7}$$

Where A is the area of the selected feature, L is the longest dimension and *P* is the perimeter. Due to its mathematical definition, the degree of splashing (D.S.) is correlated to the elongation factor (E.F.). The shape factor for a sphere would be 1.0.

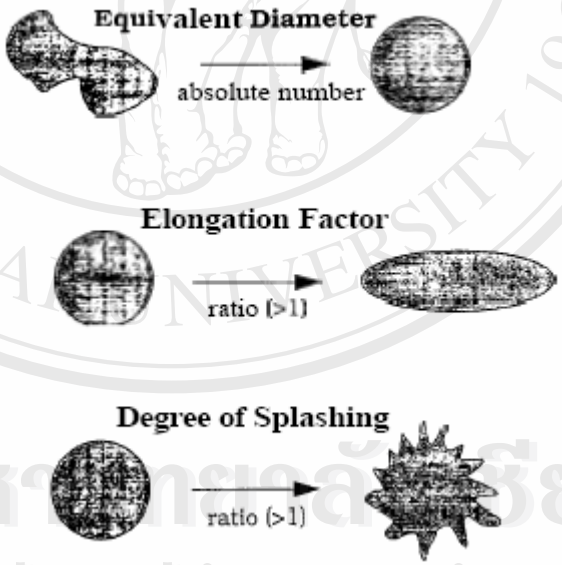

Figure 2.15 Equivalent diameter, elongation factor and degree of splashing of a selected feature [26].

Mechanical, thermo-physical, and other properties of thermally sprayed coatings are controlled by the impingement, spreading and solidification of discrete molten or semi-molten particles on a substrate or previously deposited layers [29]. However, the relationships between the parameters and the morphology of splats are not well known.

2.6 Coating characterization

2.6.1 Size distribution

The particle size may also vary over quite a wide range. To describe such situations we normally break the range up into a number of classed and try to fine out how many particles are in each size range. This range is called the particle size distribution, and it can be represented in the form of a histogram (Figure 2.16)

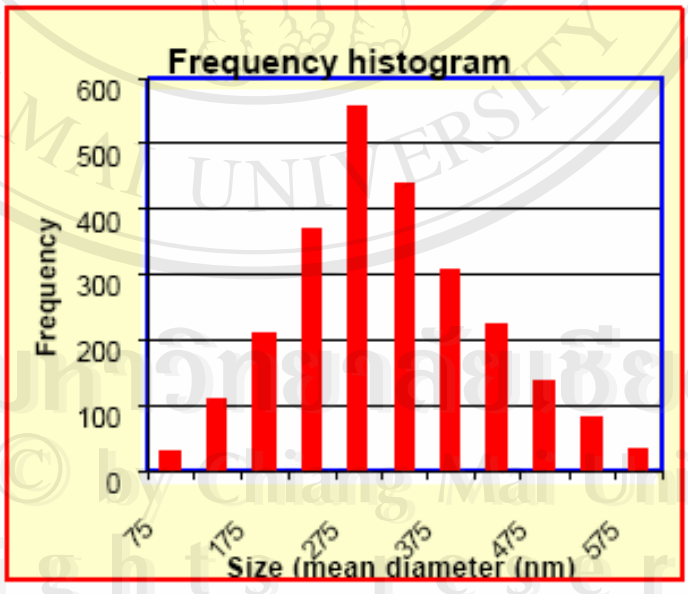

Figure 2.16 A typical particle size distribution in the form of a histogram [30].

A particle size distribution such as shown in Figure 2.16 could be obtained by counting the particle of different sizes in a microscope (or electron microscope) image. This is, however, a tedious and time consuming procedure and increasingly we seek methods of estimating the particle size distribution by indirect methods. Such procedures are two sorts.

- In some cases we separate out the different sizes and then count (or otherwise estimate) how many particles are in each size range.
- In second procedure, we try to estimate the particle distribution without first separating out the different size fraction.

The first methode is the preferred one when we have plenty of time because it can, in principle, yield the most reliable results. There are, however, many situations in which it is much better to have a reasonable estimate of the particle size distribution, especially if it can be obtained quickly.The most obvious such situation is in a flowing process stream where the particle size might be a crucial factor in determining the success of a chemical engineering process. Such situations are common in the ceramics industry, in the food processing, cosmetics manufacture and pharmaceutical industries and even in computer chip manufacture. Scientists and engineers have applied great ingenuity to the development of such particle sizing methods in recent years and there are now a number of ways of obtaining reliable estimates of PSDs in real time. It is important to recognize, however, that such methods will not normally all yield the same results when applied to a particular system. That does not mean necessarily that one is more accurate than the rest. Indeed, the only time one can expect different methods to yield exactly the same

result is when all of the particles are spherical and of the same size. Different methods measure different aspects of the distribution and sometimes, by combining results from two or more methods, one can obtain information that is not otherwise available from the individual methods [30]. The most common ways to report particle size distributions are number %. A number size distribution reflects the percentage of the particle population in different size categories [31].

The size of splats was examined using optical microscope and scanning electron microscope (SEM). Using a digital camera attached to the optical microscope, the images of splats were taken for the quantitative estimation of the diameter of individual splats. The arithmetical mean splat diameter was calculated from all splats collected for each condition.

2.6.2 Optical microscope (OM)

The microstructure characterization with an optical microscope has now become a mandatory test in any new coating development and in most coatings production. More advanced microstructural investigations can be made with the SEM (equipped with secondary electrons, back-scattered electrons. However, such a test is not always possible and the coating is most frequently characterized by its physical or chemical properties. The mechanical properties such as microhardness and wear resistance are probably the most often checked [2]. The OM technique is now used at present in nearly all spray shops and provides a source of basic information about the coating and substrate microstructure.

The light microscope is useful in a quantitative metallographical analysis. The analysis could be made with the help of an automatic image analyser (AIA), which

can be attached to the microscope. The AIA consists of setting the grey-level on the microscope picture to separate the microstructural features. The area of one feature is related to the total area of the picture by the use of suitable mathematical treatment. The AIA enables quantitative analysis of voids, which are larger than 0.5 μm (being the resolution limit for the light microscpoe). The contribution to total porosity resulting from the voids being smaller (the voids of 0.01-0.1 μm are always present in the thermally sprayed coatings) could not be found using the light microscope [2].

2.6.3 Scanning Electectron Microscope (SEM)

In the SEM an electron beam of energy up to 50 keV is focused on the surface of the sample. The electron beam ionizes the atom near to the surface and these results in an emission of secondary electrons (SE) of energy up to 50 eV, which enables surface topology to be observed. The electrons of the primary electron beam that are elastically scattered inside the sample are called backscattered electrons (BSE) and might be used to contrast the element within the coating. The back scattered electrons are moving straight and this results in an attenuation of the single coming from the holes.The surfaces of specimens for SEM investigation must be electrically conducting [2].

2.6.4 Thickness

Coating thickness measurement is an important procedure in the present research and the equipment utilised depended on whether the thickness is of the order of micron or of the millimetre range. The followting methode have been used in the

recent; Fischerscope Multi Thickness Measuring Instrument, Dial Gauge Measurement and Microscopic Measurement

In this work, the optical microscope was used to measure the average thickness of the coating. This process is a destructive means of measurement (Standard ISO 1463, 1983), which involves sectioning, mounting the cross-section, grinding and polishing the sample. In some cases etching was required to show the difference between the substrate and the coating. For any given coating thickness, measurement errors generally increase with decreased magnification, hence the highest accuracy was found when using the scanning electron microscope. The magnification was chosen so that the field of view is between 1.5 and 3 times the coating thickness, as specified in ISO 1463 (1983). Five distributed measurements were made along a deposits length in the Stokes (2003) study and the averaged, as stated in the standard ISO 2064 (1980).

2.6.5 Roughness

Surface roughness of a machined product could affect several of the product's functional attributes, such as contact causing surface friction, wearing, light reflection, heat trasmission, ability of distributing and holding a lubricant, coating and resisting fatigue [32]. Therefore, surface roughness becomes one of the important quality aspects in end-milling products.

There are various simple surface roughness amplitude parameters used in industry, such as roughness average (R_a), root-mean-square (rms) roughness (R_q) and maximum peak-to-valley roughness (R_y or R_{max}), etc. The parameter R_a is used in this study. The average roughness (R_a) is the area between the roughness profile and its

mean line, or the integral of the absolute value of the roughness profile height over the evaluation length (Figure 2.17). The average roughness (R_a) is the computed average of all deviatoins of the roughness profile from line over the defined length. R_a theoretically corresponds to the distance between several lines when above the median and valleys below the median are converted into rectandles of equal size [33]. Therefore, The roughness of the surface is usually described by the parameter R_a defined as:

$$R_a = \frac{1}{L}\int_0^L |Y(x)|dx \qquad (2.8)$$

Where

R_a = the arithmetic average deviation from the mean line

L = the sampling length

Y = the ordinate of the profile curve

There are many methods of measuring surface roughness, such as using specimen blocks by eye or fingertip, microscope, stylus type intruments, profile tracing instrument (produced by Federal Product Co.) was used in this study [34]. The profile of the surface is presented in Figure. 2.17.

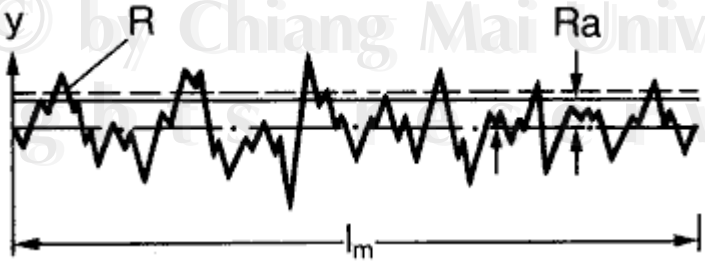

Figure 2.17 The profile of the surface [34].

2.6.6 Porosity

The thermally sprayed coatings are composed of at least two phases: porosity and solid matrix. Very often the solid matrix contains separate phases resulting from rapid solidification and cooling. The porosity can be determined with the use of the previously discussed image analysers, taking into account the limitation of this method. The porosity influences many mechanical and physical properties of coatings. Moreover, it is owing to the porosity that many properties of coatings differ from those of bulk material. Finally, the determination of the porosity in many cased enables the prediction of other properties of the sprayed material [2].

2.6.7 Hardness

Hardness is not an intrinsic material property dictated by precise definitions in terms of fundamental units of mass, length and time. A hardness property value is the result of a defined measurement procedure. The usual method to achieve a hardness value is to measure the depth or area of an indentation left by an indenter of a specific shape, with a specific force applied for a specific time. There are three principal standard test methods for expressing the relationship between hardness and the size of the impression, these being Brinell, Vickers, and Rockwell. For practical and calibration reasons, each of these methods is divided into a range of scales, defined by a combination of applied load and indenter geometry.

The term microhardness test usually refers to static indentations made with loads not exceeding 1 kg. The indenter is either the Vickers diamond pyramid or the Knoop elongated diamond pyramid. The procedure for testing is done on a microscopic scale with higher precision instruments. The surface being tested

generally requires a metallographic finish; the smaller the load used, the higher the surface finish required. Precision microscopes are used to measure the indentations; these usually have a magnification of around X500 and measure to an accuracy of $\pm$0.5 micrometres. Also with the same observer differences of $\pm$0.2 micrometres can usually be resolved. It should, however, be added that considerable care and experience are necessary to obtain this accuracy. In the Vickers diamond test, the indentor used is a pyramidal shaped diamond and the indentor is forced into the surface of the material under the action of a static load for 10 to 15 seconds. Vickers Diamond hardness number, H_D is given by

$$H_D = \frac{\text{Applied load (kg)}}{\text{Surface area of impression (mm}^2\text{)}} \qquad (2.8)$$

The standard indentor is a square pyramid shape with an angle of 136° between opposite faces as shown in Figure 2.18. One advantage of the Vickers test is that the square impressions made are always geometrically similar, irrespective of size. The plastic flow patterns, therefore, are very similar for both deep and shallow indentations and, in consequence, the hardness value obtained is independent of the magnitude of the indenting force used.

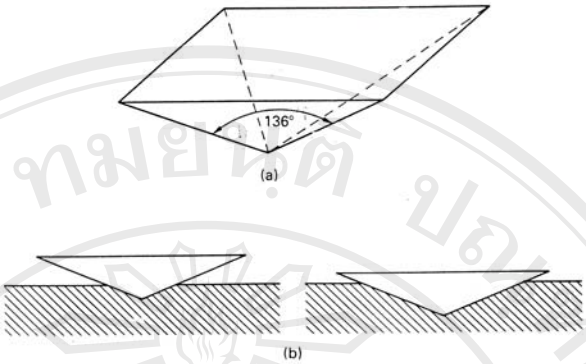

Figure 2.18 (a) Pyramid shaped diamond indentor, (b) Shallow and deep diamond impressions showing geometrical similarity [35].

After the impression has been made, the size of the impression is measured accurately using a microscope. Some hardness testing machines use an alternative system in which a magnified image of the impression is projected onto a screen and the size of this image measured, either with reference to a graticule inscribed on the screen or with a special rule. Both diagonals of the impression are mearsured and the mean value of D, the diagonal lenght, is used in the determination of the hardness number.

$$H = \frac{2F\sin\theta/2}{D^2} \qquad (2.9)$$

Where $\theta = 136°$, giving

$$H_D = \frac{1.8544F}{D^2} \qquad (2.10)$$

Where *F* is the applied load in mg , and D is the mean diagonal length in μm.

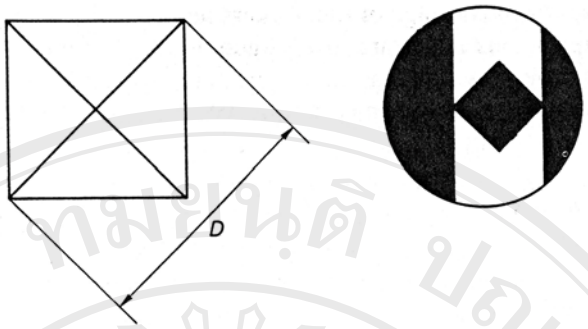

(a) (b)

Figure 2.19 (a) Vickers diamond impression, (b) View through microscopes of Vickers machine [35].

The microscope of the standard Vickers hardness test machine has a pair of micrometer shutters built into the eyepiece. The shutters are adjusted untill the impression is exactly bracketed between them (Figure 2.19). The distance between the shutter is indicated on a digital counter attached to the eyepiece. The reading on this counter is termed the ocular reading and a set of tables is provided with the machine to convert the ocular reading into diamond hardness number, H_D, for a range of indenting loads. The ocular reading can be read to an accuracy of ±0.001 mm. For the most accurate hardness results, the indenting laod sohld be adjusted to give impressions with a diagonal length of about 0.5 mm.

There are systems avaliable for microhardness testing and the two most widely-used methods are the Vickers Damond test and the Knoop Diamond test. The principle of the Vickers Diamond microharness test is basically the same as for the standard Vickers test but indenting loads used are measured in grams rather than kilograms. This type of hardness testing is performed on a metallurgical microscope

adapted for the purpose. The small pyramidal diamond indentor is embeded in the surface of a special objective lens. The surface of the test sample is prepared to a high polish and etched for micro-examination. When view under the microscope with a high magnification, usually some value between × 200 and × 200, any particular micro-constituent of feature can be centred in the field of view and micro-sized diamond indentation made using a small indenting load. The load used is usually of some value between 1g and 100g. The full load is normally applied for 10 to 15 seconds. The size of the square indentation is then carefully measured and the mean length of the diagonals, D, used to determine the hardness possible with a typical microscope attachment is of the order of ± 0.0001 mm [35].

2.7 Wear

Wear is a process of removal of material from one or both of two solid surfaces in solid-state contact. It occurs when solid surfaces are in sliding or rolling motion relative to each other. In well-designed tribology systems, the removal of material is usually a very slow process, but it is very steady and continuous.

2.7.1 Wear mechanism

The mechanism of wear is very complex and the theoretical treatment without the use of rather sweeping simplifications is not possible. It should be understood that the real area of contact between two solid surfaces compared with the apparent area of contact is invariably very small, being limited to points of contact between surface asperities. The load applied to the surfaces will be transferred through these points of contact and the localised forces can be very large. The material intrinsic surface

properties such as hardness, strength, ductility, work hardening etc. are very important factors for wear resistance, but other factors like surface finish, lubrication, load, speed, corrosion, temperature and properties of the opposing surface etc. are equally important

The classification of wear processed based on the type of wearing contacts such as single phase and multiple phase. In single-phase wear, a solid, liquid, or gas moving relative to sliding surface cause material to be remove from the surface. The relative motion may be sliding (unidirectional) or rolling. In multiple-phase wear, wear also results from a solid, liquid, or gas moving across a surface, but in this case, solid, liquid, or gas act as a carrier for a second phase (particle, asperity, liquid drop, and gas bubble) that actually produce the wear. Wear is classified into six categories, which are base on quite distinct and independent phenomena, as follows:

2.7.1.1 Abrasive wear

Abrasive wear may be described as damage to a surface by a harder material. In the abraive wear process, asperities of the harder surface press into the softer surface, which plastic flow of the softer surface occuring around the asperities from the harder surface. When a tangential motion is imposed, the harder surface removes the softer material by combined effects of microploughing, microcutting, and microcracking. There are two general situations in which this type of wear occurs. In the first case, the hard surface is the harder of two rubbing surfaces (two-body abrasion) as shown in Figure 2.20 (a), e.g., in mechanical operations such as griding, cutting, and machining. In the second case, the hard surface is a third body, generally a small particle of grit or abrasive, caught between the two other surfaces and

sufficiently harder than they are to abrade either one or both of them (three-body abrasion) as shown in Figure 2.20 (b) [10].

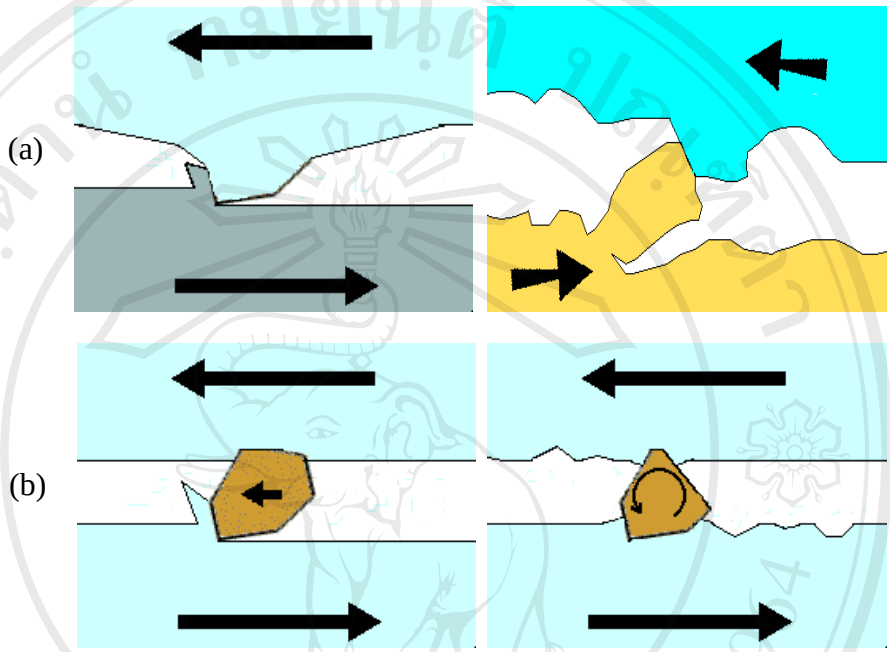

Figure 2.20 Schematic of abrasive wear phenomena.

(a) two-body abasive, (b) three-body abrasive [9]

2.7.1.2 Adhesive wear

Adhesive wear is often called galling or scuffing, where interfacial adhesive junctions lock together as two surfaces slide across each other under pressure [12]. As normal pressure is applied, local pressure at the asperities become extremely high. Often the yield stress is exceeded, and the asperities deform plastically until the real area of contact has increased sufficiently to support the applied load, as shown in Figure 2.21. In the absence of lubricants, asperities cold-weld together or else junctions shear and form new junctions. This wear mechanism not only destroys the

sliding surfaces, but the generation of wear particles which cause cavitation and can lead to the failure of the component. An adequate supply of lubricant resolves the adhesive wear problem occurring between two sliding surfaces.

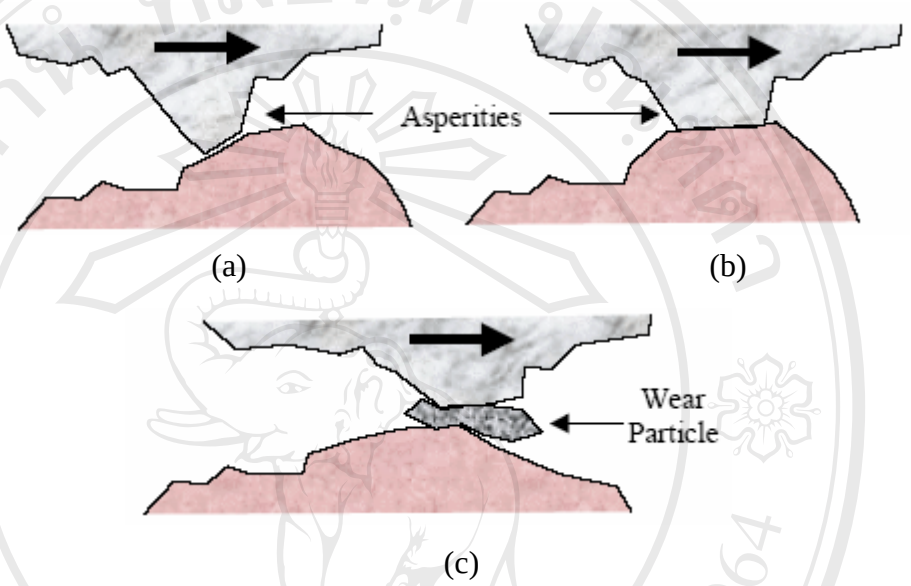

Figure 2.21 Schematic of generation of a wear particle as a result of adhesive wear process [10].

2.7.1.3. Corrosion wear

Corrosion wear can be explained in terms of the dynamic interaction between environment and mating material surfaces plays a significant role. This interaction gives rise to a cyclic stepwise process. In the first step, the contacting surfaces react with enviroment, and reaction product are formed on the surface. In the second step, attrition of the products occurs as result of crack formation and/or abrasion in the contact interactions of the matetrials. The process results increased reactivity of the asperities because of increased temperature and changes in the mechanical properties of asperities [12].

2.7.1.4. Fatigue wear

Fatigue occurs when two sliding surface come into contact, asperities on the softer surface are deformed by repeated loading to generate a relatively smooth surface. Eventually, with asperities-plane contacts, the softer surface experiences cyclic loading as the asperities of the harder surface plough through it. Surface friction by the harder asperities on the softer surface induces plastic shear deformation that accumulates with repeated loading. As the subsurface deformation continues, cracks are nucleated below the surface. These cracks initiate from the point where the shear stress is maximum, and propagate to the surface as shown in Figure 2.22. Further loading causes the cracks to propagate parallel to surface. When these cracks finally intercept the surface, long, thin wear sheets delaminate, giving rise to platelike particles. Materials are rarely perfect, hence the exact position of ultimate failure is influenced by inclusions, porosity, microcracks and other factors. Fatigue failure requires a given number of stress cycles and often predominates after a component has been in service for a long period of time [10].

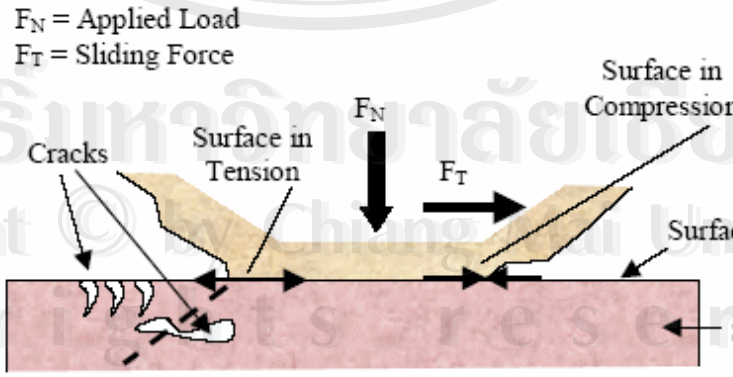

Figure 2.22 Schematic of fatigue wear, due to the formation of surface and subsurface cracks [10].

2.7.1.5. Fretting wear

When components are subjected to very small relative vibratory movements at high frequency, an interactive form of wear, take place that is initiated by adhesion, is amplified by corrosion, and has its main effect by abraion. Fretting wear frequently occurs between components that are not intented to move. Surfaces subjected to fretting have a characteristic appearance, with red-brown patches on ferrous metals and adjacent areas that are highly polished as a result of lapping by the hard iron oxide debris. It is observed that the environment plays a strong role in the wear of surfaces that undergo fretting.

2.7.1.6. Erosion wear

Erosion of materials and components caused by the impingement of solid particles or small drope of liquid or gas can be a life-limiting phenomenon for systems in erosive environments. The basic mechanism involved is depicted schematically in Figure.2.23. As a result of the impact in solide-state contact of a particle of material with the solid surface, part of the surface of material is removed. The particle itself can very in composition as well as in form. The response of engineering materials to the impingement of solide particles varies greatly depending on the class of material, the state of materials to which those, materials have been exposed, and the environmental parameters associated with the erosion process, such as impact velocity, impact angle and particle type and size.

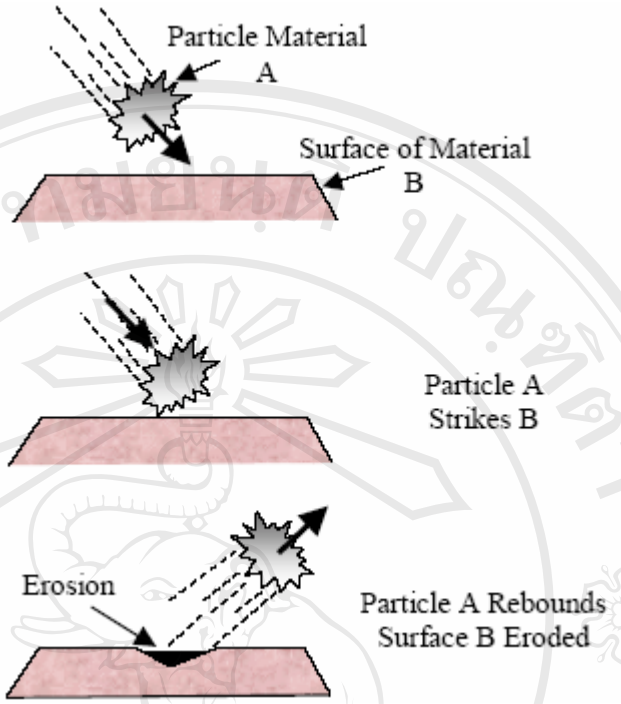

Figure 2.23 Schematic of erosion wear [10].

2.7.2 General observations

Mass loss measurements from wear tests were used to plot total mass loss against time. The relationship was generally linear and wear rate was found from the gradient determined by least squares analysis. The estimated wear rates could then be used to find the two wear coefficients from the two forms of the Archard equation given by expressions (2.11) and (2.12):

$$Q = KW/H \qquad (2.11)$$

$$Q = kW \qquad (2.12)$$

Where Q is the wear rate; W the applied load; H the hardness of the wear specimen; K the dimensionless wear coefficient and k is the dimension wear coefficient [35].

2.7.3 Thermal spray coating for wear resistance

Coating the worn surface of a material using thermal spraying increases the surfaces wear resistance. Materials in their wrought or cast form (for example stainless steel) are generally less wear resistant than those coated thermally (stainless coated with stainless steel) [36], due to the temperature effects experienced during spraying, resulting structure and porosity levels. Porosity enables small amounts of lubricant to collect within the voids, therefore friction loss rates are lower as a result. On the other hand substrates with low wear resistance can be coated with a thin film of a high wear resistant coating (such as tungsten carbide-cobalt), to allow the component operate in a harsh environment [37].

In 1996, D.J. Whitefield and A. Van Bennekon evaluated the wear properties of metastable duplex Cr-Mn-N alloys under impact abrasive wear conditions. The results of the impact abrasive wear tests showed that the wear rates of the experimental alloys were similar to those of SAF2205, while after heat treatment all of the experimental alloys were slightly more resistant to were than SAF2205. The lowest resistance to impact abrasive wear was displayed by the 3CR12 alloy, with the heat-treated experimental alloys being as much as 2.5 times more resistant to wear under these conditons. The increased wear resistance was found to be due to the effects of work hardening and increased austenite phase percents, brought about by the heat-treatment process[38].

2.8 Review of previous work

In 2000, Helene Ageorges and Pierre Fauchais studied the stainless steel particles used in plasma spraying by examing sprayed particles in mid-flight and their

resulting splats and coatings. The results show that the splats of powder are extensively fingered and become circular. In this work, stainless steel particles have been plasma sprayed. For particles in the size range 50-80 μm, and a mean size of 65 μm. The morphology of splats, collected on smooth stainless steel substrate are extensively fingered.The polished cross sections of coatings exhibit a lamellar structure. The microhardness, measured with a 5 N load of pure stainless steel deposits (270 ± 22 Hv). The surface roughness of coatings is R_a= 10.5 ± 0.8 μm [39]. Then, Dallaire manufactured coatings by arc spraying with new core wires. The coatings produced with the new cored wire are at 10 times more abrasion resistant than coatings produced by arc spraying commercial cored wires. These arc sprayed coatings possess abrasion wear resistances that considerably surpass those of structural materials and commercial arc sprayed coatings. The arc sprayed coating is expected to find applications in numerous industrial sectors [40].

FeCrAl coatings were deposited with arc spraying process and their characteristics were quantitatively determined by Giumin Liu in 2001. Observations of the surface morphology of the coatings were conducted in a scanning electron microscope (SEM). The surfaces of arc spraying FeCrAl coatings reveal cauliflower-shaped with diameters ranging from 30 to 100 μm. The arc spray coatings are compose by FeCr, AlFe and the aluminium oxide (Al_2O_3). There are three different layers in arc spraying coating: porous, dense and outer layer. Microhardness values of the coatings and the substrate as a function of the distance along the direction perpendicular to the coating-substrate interface were measured. The average value of the microhardness of arc sprayed coating is small. The profile roughness coefficients of the coatings and substrates were also measured. When the thickness of FeCrAl

coating is 400 μm, the profile roughness coefficient values of the coating show no mutuality with that of the coating-substrate interface. Whereas when the thickness of coating is less than 50 μm, a linear relationship between the profile roughness vaules of coating and interface has been obtained. This suggests that the morphology of the substrate has a ditrect effect on that of its bonding coating surface topology when the coating is relatively thin [41]. In the following year, H. Pokhmurska produced new coatings with low porosity and small grains by arc spraying of FeCrB+Al and FeCr+Al+C powder wire in a steel cover. Wear tests with the block-on-ring configuration at boundary lubrication and friction under normal pressure at 5 Mpa have been performed. Results for sprayed coatings of both systems showed their high wear resistance. The powder wires for both these systems are currently produced and widely used for restoring the high loaded worn out friction units (crankshafts of engines, compressors, pumps, etc.) [42].

In 2003, G. Jandin investigated mechanical properties of steel coatings built with a twin wire arc spray system. Relationships between spray parameters, microstructure and corresponding hardness of the coatings were determined. Some correlations were made between these properties, spraying conditions and the microstructure of the deposits. The direct relationships do exists between spray conditions, oxide content in the coating and microhardness. When increasing the compressed air flow rate, smaller particles and finer lamellae were made and its decreases later because of a higher oxide content. The atomizing gas spray flow rate has also a main influence on the oxide content: the lower the air flow rate, the lower the oxide content. Higher oxide content leads to a higher hardness; better carbon

retention allows an increase in hardness for a given oxide content. Splat thickness and oxide content depend on the spraying conditions [43].

According to properties of thermally sprayed coatings are controlled by various parameters of spraying process. In 2004, thermal spraying technique with significantly different parameters was examined by S. Sampath. In-flight particle diagnostics was performed; Ni-5wt.%Al splats and deposits were fabricated and analyzed. Porosity of the deposits were evaluated and correlated to the process variables. The study examined the effect of spray parameters on the microstructure and properties of coatings. Different spray parameters were examined for a single material namely Ni-5wt%Al. Thermal energy controlled the flattening behavior of the particles forming the splats. The high in-flight velocity alone led only to a seemingly dense structure. For wire arc sprayed coating this was not surprising considering the comparatively high porosity of these deposits. This study provides a framework for enhanced understanding of the phenomena that occur during thermal spray deposition of metallic alloys [44].

Later on, M.P. Planche studied the influence of input parameters on the relationships between impact mode and coating properties by using in-flight particle characteristics at the spraying distance. Various input parameters were tested in order to point out their influence on particle characteristics. It has been shown that atomizing gas flow rate clearly has a main influence on particle characteristics in the studied range of parameters: the higher the flow rate, the smaller and the quicker the particles. At further spraying distances, velocity and temperature of particles decrease but size is maintained constant. The morphology of the splats has been studied in terms of flattening degree and shape factor. As consequence, flattening degree and

splashing level increase with flow rate. Finally, some correlations have been established between input parameters and properties of coatings in relation with particle characteristics and splats analysis. Particle characteristics have been connected to coating properties and strong tendencies have been noticed. A main interaction exists between gas flow rate and coating properties. While increasing gas flow rate, particle velocities increase as their diameter decrease leading together to an increase of hardness of the deposit. Concerning the oxide content, this value increases with the gas flow rate which is consistent with what could generally be observed. The specific surface of the particles in contact with oxygen increases and causes an increase of the oxide content. It has been noted simultaneously a decrease of the porosity due to a greater flattening of the particles and a better accommodation of the particles between themselves.[5]

In 2005, the analysis of atomizing particles collection and particle size distribution is favorable for splashing and flattening research. Atomizing particles are in shape of sphere generally during arc spraying stainless steel. With an increase of atomizing pressure, in-flight particles exhibit properties, such as fully atomizing, uniform and fine particle size, higher flight velocity and better splat. The results show deposit possesses good density, high hardness and low porosity. The wear resistance of the coating is greatly improved. Therefore, it is important to establish relationships among spray parameters, behaviors of atomizing particles, morphological aspect of splat formation and coating generation by examining droplets forming process during spraying. The results are propitious to optimize the coating quality of arc spray forming [45].

H.L. Liao investigated particle properties of individual electrodes of the arc spray process by separating particles from the anode and the cathode wires. A particle size distribution was found for particles from each wire. This particle size distribution is probably due to the periodical fluctuation of the arc length and the arc voltage leading to a varying particles size. In addition, after atomization the difference average diameter particle between from the anode and the cathode becomes quite small and the difference can be reduced by increasing atomizing gas pressure. Microstructure analysis also indicates that the closed nozzle system with a converging-diverging orifice (CD/CL) nozzle tends to produce coating with finer microstructure, lower porosity and higher oxide content, than the open nozzle which leads to very coarse coating microstructure with high porosity but low oxide content because of its poorer atomizing performance. Analysis of the gas dynamic performance of the different nozzles and numerical prediction of the splat diameter distribution were also conducted. They show that one of the major drawbacks of an open nozzle system is its relatively longer distance between the wires intercept point and the nozzle exit where the gas velocity combined with the experimental particle size distribution in the coating sprayed by using different nozzle. Results show a smaller average splat diameter and a narrower splat diameter distribution for CD/CL nozzle that is in close agreements with the microstructure analysis. It was found that a major disadvantage of the open nozzle system is its relatively longer distance between the wires interception point and the nozzle exit where the gas velocity attains its maximum value [46].